

# Less Is More: a Mutation in the Chemical Defense Pathway of *Erysimum cheiranthoides* (Brassicaceae) Reduces Total Cardenolide Abundance but Increases Resistance to Insect Herbivores

Mahdieh Mirzaei<sup>1</sup> · Tobias Züst<sup>2</sup> · Gordon C. Younkin<sup>1</sup> · Amy P. Hastings<sup>3</sup> · Martin L. Alani<sup>1</sup> · Anurag A. Agrawal<sup>3</sup> · Georg Jander<sup>1</sup>

Received: 26 April 2020 / Revised: 6 October 2020 / Accepted: 9 October 2020 © Springer Science+Business Media, LLC, part of Springer Nature 2020

### **Abstract**

Erysimum cheiranthoides L (Brassicaceae; wormseed wallflower) accumulates not only glucosinolates, which are characteristic of the Brassicaceae, but also abundant and diverse cardenolides. These steroid toxins, primarily glycosylated forms of digitoxigenin, cannogenol, and strophanthidin, inhibit the function of essential Na<sup>+</sup>/K<sup>+</sup>-ATPases in animal cells. We screened a population of 659 ethylmethanesulfonate-mutagenized E. cheiranthoides plants to identify isolates with altered cardenolide profiles. One mutant line exhibited 66% lower cardenolide content, resulting from greatly decreased cannogenol and strophanthidin glycosides, partially compensated for by increases in digitoxigenin glycosides. This phenotype was likely caused by a single-locus recessive mutation, as evidenced by a wildtype phenotype of F1 plants from a backcross, a 3:1 wildtype:mutant segregation in the F2 generation, and genetic mapping of the altered cardenolide phenotype to one position in the genome. The mutation created a more even cardenolide distribution, decreased the average cardenolide polarity, but did not impact most glucosinolates. Growth of generalist herbivores from two feeding guilds, Myzus persicae Sulzer (Hemiptera: Aphididae; green peach aphid) and Trichoplusia ni Hübner (Lepidoptera: Noctuidae; cabbage looper), was decreased on the mutant line compared to wildtype. Both herbivores accumulated cardenolides in proportion to the plant content, with T. ni accumulating higher total concentrations than M. persicae. Helveticoside, a relatively abundant cardenolide in E. cheiranthoides, was not detected in M. persicae feeding on these plants. Our results support the hypothesis that increased digitoxigenin glycosides provide improved protection against M. persicae and T. ni, despite an overall decrease in cardenolide content of the mutant line.

 $\textbf{Keywords} \ \textit{Erysimum cheiranthoides} \cdot \text{Cardenolide} \cdot \text{Na}^+/\text{K}^+\text{-ATPase} \cdot \textit{Trichoplusia ni} \cdot \textit{Myzus persicae} \cdot \text{Resistance} \cdot \text{Plant defense}$ 

# Introduction

Plants produce a wide array of specialized metabolites as chemical defenses against insect herbivory. Although some individual compounds can be broadly effective, greater

- Georg Jander gj32@cornell.edu
- Boyce Thompson Institute, 533 Tower Rd, Ithaca, NY 14853, USA
- Institute of Plant Sciences, University of Bern, Altenbergrain 21, CH-3013 Bern, Switzerland
- Department of Ecology and Evolutionary Biology, Cornell University, Ithaca, NY 14853, USA

Published online: 12 November 2020

chemical diversity has been shown to provide enhanced protection against a variety of herbivores. For example, a detailed study of 31 sympatric tree species from the monophyletic clade Protieae (Burseraceae) showed that an increased diversity of chemical defenses, including procyanidins, flavone glycosides, chlorogenic acids, saponins, triterpenes and sesquiterpenes, was associated with enhanced herbivore resistance (Salazar et al. 2018).

Diversity of chemical structures, even if they belong to the same metabolic class, can provide defensive advantages. In some cases, compounds with similar structures and the same metabolic target site may act synergistically in defense against individual herbivore species. For instance, although they have comparable photosensitizing functions, six fourancoumarins

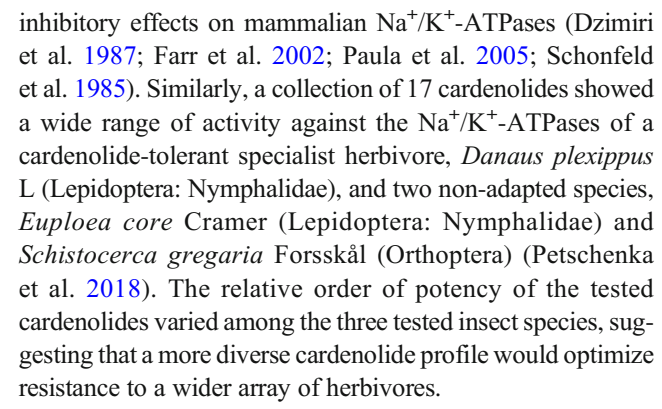


from Pastinaca sativa L (Apiaceae) provided enhanced defense against Helicoverpa zea (Lepidoptera: Noctuidae; formerly Heliothis zea) relative to each compound individually (Berenbaum et al. 1991). Alternatively, a more varied chemical arsenal could be evolutionary advantageous if variants of the same chemical structure differ in their toxicity towards multiple herbivore species. In Arabidopsis thaliana L (Brassicaceae), which produces both tryptophan-derived indole glucosinolates and methionine-derived aliphatic glucosinolates, indole glucosinolates provide better protection against Myzus persicae Sulzer (Hemiptera: Aphididae; green peach aphid) (Kim et al. 2008). Conversely, growth of Trichoplusia ni Hübner (Lepidoptera: Noctuidae; cabbage looper), a generalist lepidopteran herbivore, was more strongly impacted by aliphatic rather than indole glucosinolates in A. thaliana mutant lines (Müller et al. 2010). Performance of the crucifer-feeding specialist Pieris rapae L (Lepidoptera: Pieridae; white cabbage butterfly), which has a high level of glucosinolate tolerance due to chemical diversion of the breakdown products (Wittstock et al. 2004), was not improved by the loss of either indole or aliphatic glucosinolates in A. thaliana (Müller et al. 2010).

Erysimum cheiranthoides L (Brassicaceae; wormseed wallflower), a widely distributed annual species, accumulates not only indole and aliphatic glucosinolates, but also cardenolides, steroid-derived specialized metabolites that function as inhibitors of essential Na<sup>+</sup>/K<sup>+</sup>-ATPases in animal cells (Züst et al. 2020). This additional set of defensive compounds provides enhanced protection against cruciferspecialist herbivores that can tolerate or detoxify glucosinolates, including the glucosinolate-tolerant *P. rapae* (Dimock et al. 1991; Renwick et al. 1989; Sachdev-Gupta et al. 1993; Sachdev-Gupta et al. 1990).

Cardenolides and structurally related bufadienolides, which also inhibit Na<sup>+</sup>/K<sup>+</sup>-in animal cells, are produced by at least a dozen plant families (Agrawal et al. 2012). Like glucosinolates, for which more than 120 different compounds have been identified across the Brassicaceae (Fahey et al. 2001), cardenolides are a large group of chemically and functionally similar plant defensive metabolites. A recent analysis identified a total of 95 different cardenolide structures in 48 species of the Erysimum, the only cardenolide-producing genus within the Brassicaceae (Züst et al. 2018; Züst et al. 2020). This vast diversity is primarily generated by modifications to the core steroid structure of the molecules (the genin), and by glycosylation of the genin with various sugar moieties to form linear glycoside 'tails'. In E. cheiranthoides, the first Erysimum species to have its genome sequenced (Züst et al. 2020), the most abundant cardenolides are glycosides of the three genins digitoxigenin, cannogenol, and strophanthidin (Fig. 1).

Several in vitro studies have demonstrated that modifications of the core steroid structure of cardenolides alter the



In vitro enzyme inhibition assays provide only a partial view of the effects that cardenolides have when they are consumed by insect herbivores. For instance, efflux pumps and barriers to diffusion that prevent movement of cardenolides into the nervous system of some insect species (Groen et al. 2017; Petschenka et al. 2013) would not be relevant in an in vitro Na<sup>+</sup>/K<sup>+</sup>-ATPase inhibition assay. To initiate an investigation of the in vivo role of cardenolide diversity in defense against insect herbivores, we conducted an E. cheiranthoides mutant screen to identify plants with altered cardenolide profiles. We characterized the genetic basis and biochemical phenotype (cardenolides and glucosinolates) of a mutant line with lower cardenolide content, but altered composition favoring digitoxigenin glycosides. We used this mutant to further characterize susceptibility of two generalist herbivores to cardenolide classes and report on the accumulation of these compounds in insect bodies. In sum, this work lays the foundation for understanding the biochemical genetics of cardenolide biosynthesis and their impacts on a diverse community of herbivores.

### **Methods and Materials**

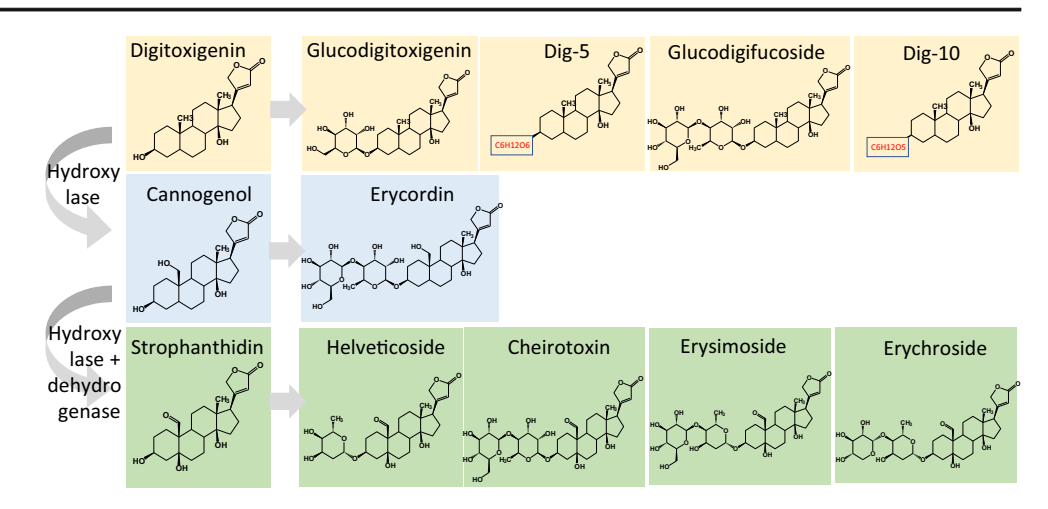
**Experimental design** Fig. S1 shows a flow chart of the experiments that were conducted. Supplemental Data File S1 contains the raw data for all figures shown in this manuscript.

Plant, Insects, and Growth Conditions We conducted all experiments with the genome-sequenced *E. cheiranthoides* var. Elbtalaue (Züst et al. 2020), Arabidopsis Biological Resource Center (https://abrc.osu.edu) accession number CS29250. Plants were grown in Cornell Mix (by weight 56% peat moss, 35% vermiculite, 4% lime, 4% Osmocote slow-release fertilizer [Scotts, Marysville, OH], and 1% Unimix [Scotts]) in Conviron (Winnipeg, CA) growth chambers with a 16:8 photoperiod, 180 μM m<sup>-2</sup> s<sup>-1</sup> photosynthetic photon flux density, 60% humidity, and constant 23 °C temperature.

We obtained *Trichoplusia ni* eggs from Benzon Research (www.benzonresearch.com) and hatched them on artificial diet (Southland Products, http://www.southlandproducts.net)



Fig. 1 Structures of cardenolides found in *Erysimum* cheiranthoides. Predicted enzymes that would convert digitoxigenin to strophanthidin and then cannogenol are shown. Digitoxigenin-, cannogenol-, and strophanthidin-derived cardenolides are highlighted in yellow, blue, and green, respectively



in an incubator at 28 °C. We started a *P. rapae* colony with approximately 30 adults that were collected on the Cornell University campus in August, 2019, and maintained this colony on *Brassica oleracea* L (Brassicaceae) cv. Wisconsin Golden Acre under the same growth chamber conditions as those used for *E. cheiranthoides*. *Myzus persicae* were from a lab colony of a previously described "USDA" strain (Ramsey et al. 2014; Ramsey et al. 2007), which we maintained on *Nicotiana tabacum* L (Solanaceae) in a growth room with a 16:8 photoperiod and constant 23 °C temperature.

Mutagenesis We performed ethyl methanesulfonate (EMS) mutagenesis as described previously for experiments with A. thaliana (Jander et al. 2003). Briefly, we soaked 10 g inbred line Elbtalaue seeds (approx. 48,000 seeds) in 40 ml of 100 mM pH 7.5 phosphate buffer in a 50 ml plastic tube and stored overnight at 4 °C. After decanting the buffer, we added 40 ml of fresh 100 mM phosphate buffer with 0.6% EMS (Sigma-Aldrich, St. Louis, MO) to the tube. We incubated the mixture at 23 °C for seven hours with gentle shaking. Seeds were rinsed 20 times with distilled water prior to planting in ten  $25 \times 50$  cm nursery flats. After 15 weeks, we harvested M2 seeds as ten separate pools, one from each flat. Approximately 100 M2 seeds from each pool of M1 plants were planted in individual 100 cm<sup>3</sup> pots. After four weeks, we took five 0.5 cm hole punches from mature leaves as samples for cardenolide analysis from ~70 M2 plants grown from each of the 10 pools, a total of 659 plants. We analyzed foliar cardenolides of each M2 plant by UPLC-MS as described below. For individual mutant lines with divergent cardenolide phenotypes, we confirmed consistent expression by measuring cardenolides in five additional leaf samples of the same plant, and compared the results with two-tailed t-tests to 12 wildtype samples, considering P < 0.05 to be a significant difference. We back-crossed confirmed mutant plants to wildtype Elbtalaue and analyzed six F1 plants by UPLC-MS, comparing their cardenolide profile to six M2 mutant and six wildtype plants. A single F1 plant was then selected

for propagation, and F2 progeny of this plant were used for further experiments. In the F2 generation, we measured cardenolides and glucosinolates in 7 individual homozygous mutant plants and compared results to sibling plants with a wildtype cardenolide phenotype using two-tailed t-tests, considering P < 0.05 to be a significant difference.

Bulked-Segregant Analysis Coupled to Whole Genome **Sequencing** We collected tissue samples from 44 mutant and 155 phenotypically wildtype siblings (as measured by HPLC-MS) from an F2 mapping population. Three 0.5 cm hole punches of mature leaves from each plant were pooled to ensure equal representation of individuals. We extracted DNA from the both tissue pools using the Wizard® Genomic DNA Purification Kit (Promega, Madison, WI) following the manufacturer's instructions. DNA libraries were prepared by the Cornell University Genomics Facility using the TruSeq PCR free prep kit according to the manufacturer's instructions (Illumina, San Diego, CA). DNA libraries were sequenced using an Illumina NextSeq500 instrument (75 bp single end reads) in the Biotechnology Resource Center of Cornell University. Sequencing data were submitted to the Sequence Read Archive (https://www.ncbi.nlm.nih.gov/sra) as data set SRP286204. Raw reads were aligned to the E. cheiranthoides var. Elbtalaue genome (Züst et al. 2020; www.erysimum.org) using Burrows-Wheeler Aligner version 0.7.8 (Li and Durbin 2009), and the resulting BAM file was sorted using samtools (Li et al. 2009) and indexed using Picard (https://broadinstitute.github.io/picard/). We used samtools mpileup and beftools call (Li 2011) to create a pileup of the aligned reads and call variants, with a minimum base quality of 20 and minimum mapping quality of 40. We also filtered variants to keep only single nucleotide polymorphisms with a quality score greater than 50 and a read depth between 20 and 250. We used R (R Core Team 2020) with dplyr (Wickham et al. 2020) to calculate and plot the moving median of mutant allele frequencies over a window of 1 Mpb.



Cardenolide Assays We weighed ground frozen leaf tissue, 50-100 mg per sample, into 2 ml tubes. After addition of four 3-mm stainless steel balls (Abbott Ball Company, Hartford, CT) to each tube, the samples were homogenized for  $2 \times$ 2 min at using a Harbil 5G-HD shaker (Fluid Management, Wheeling, IL) and kept frozen in liquid nitrogen until extraction. Three times tissue volume of methanol: formic acid (99.8%: 0.2%) were added. We vortexed samples vigorously for 10 s, centrifuged them for 30 s at 400 g, sonicated them in an ultrasonic bath for 30 min, and then centrifuged them again for 30 s at 400 g. We then centrifuged the extracts for 10 min at 20,000 g and transferred the supernatants to glass HPLC vials for LCMS analysis using a Q-Exactive hybrid quadrupole-orbitrap mass spectrometer (Thermo Scientific) equipped with a Titan<sup>TM</sup> C18 UHPLC Column, (100 × 2.1 mm, particle size 1.9 µm; Sigma-Aldrich). Two or three ul injections were separated using the following linear gradient: mobile phase B (100% acetonitrile plus 0.1% formic acid) increased from 2 to 97% over 10 min, held at 97% for 1.5 min, and returned to 98% mobile phase A (0.1% formic acid in water) for equilibration for 1.5 min. The flow rate of the mobile phases was 0.5 ml/min, and the column temperature and the autosampler temperature were maintained at 40 °C and 15 °C, respectively. Eluted compounds were detected from 200 to 800 m/z with 140,000 resolution (full width at half maximum, at m/z 200) in positive and negative ion modes.

We quantified the relative abundance of cardenolide compounds by isolating the following positive-ion chromatograms: cheirotoxin (C35H52O15), rt. = 3.93 min, [M + $H^{+}_{z} = 713.3384 \text{ m/z}$ ; erysimoside (C35H52O14), rt. =  $4.06 \text{ min}, [M + H]^+ = 697.3435 \text{ m/z}; \text{ erychroside}$ (C34H50O13), rt. = 4.2 min,  $[M + H]^+ = 667.3329$  m/z; helveticoside (C29H42O9), rt. = 4.65 min,  $[M + H]^+$  = 535.2907 m/z,; digitoxigenin (C23H34O4), rt. = 5.8 min,  $[M + H]^{+} = 375.2535 \text{ m/z}$ ; glucodigitoxigenin (C29H44O9), rt. = 4.46 min,  $[M + H]^+ = 537.3063 \text{ m/z}$ ; dig-5 (C29H44O9), rt. = 4.55 min,  $[M + H]^+ = 537.3063$  m/z; glucodigifucoside (C35H54O13), rt. = 4.7 min,  $[M + H]^+$  = 683.3642 m/z; dig-10 (C29H44O8), rt. = 5.09 min, [M+  $H^{+} = 521.3114 \text{ m/z}$ ; erycordin (C35H54O14), rt. = 4.15 min,  $[M + H]^+ = 699.3592 \text{ m/z}$ . In assays of insect samples, the sodium adducts of two cardenolides, cheirotoxin  $[M + Na]^{+} = 735.3187 \text{ m/z}$  and helyeticoside  $[M + Na]^{+} =$ 557.2721 m/z, were the most abundant and were used for relative quantification. We quantified the relative abundance of glucosinolate compounds by isolating the following negative-ion chromatograms: indol-3-ylmethyl glucosinolate  $(C16H20N2O9S2; I3M), rt. = 1.85 min, [M-H]^- =$ 447.0532 m/z; 4-methoxy-indol-3-ylmethyl glucosinolate  $(C17H22N2O10S2; 4MOI3M), rt. = 2.36 min, [M-H]^- =$ 477.0638 m/z; 4-hydroxy-indol-3-ylmethylglucosinolate  $(C16H20N2O10S2; 4OHI3M), rt. = 0.9 min, [M-H]^- =$ 463.0484 m/z; 3-methylsulfinylpropyl glucosinolate (C11H21NO10S3; 3MSIP), rt. = 0.56 min, [M-H]<sup>-</sup> = 422.0249 m/z; 3-methylsulfonylpropyl glucosinolate (C11H21NO11S3; 3MSOP), rt. = 0.55 min, [M-H]<sup>-</sup> = 438.0196 m/z; 4-methylsulfonylbutyl glucosinolate (C12H23NO11S3; 4MSOP), rt. = 0.58 min, [M-H]<sup>-</sup> = 452.0360 m/z; N-methylbutyl glucosinolate (C12H23NO9S2; NMB), rt. = 1.8 min, [M-H]<sup>-</sup> = 388.0739 m/z.

We purchased digitoxigenin (Sigma-Aldrich), K-strophanthin (a mixture of cymarin, erysimoside, helveticoside, strophanthidin, k-β-strophanthin, and k-strophanthoside; Sigma-Aldrich), and helveticoside (Cfm Oskar Tropitzsch GmbH, Germany) for use as standards. We validated the remaining compounds using ms/ms analysis and comparison to known *E. cheiranthoides* cardenolide structures. The resulting raw LC/MS files were uploaded into XCMS online (https://xcmsonline.scripps.edu/) and processed for untargeted metabolomics profiling using predefined parameter sets for the UPLC/Q-Exactive system. The normalized targeted mass features corresponding to cardenolides and glucosinolates were then isolated from the output file.

We performed an HPLC-UV assay to quantify the absolute amount of cardenolides in phenotypically wildtype and mutant plant samples (F2 progeny from 454 x Elbtalaue, with phenotypes confirmed by HPLC-MS) with seven biological replicates. Ten mg freeze-dried ground plant tissue was weighed into a screw cap tube with ~30 zirconia/silica beads (2.3 mm; BioSpec Products, Bartlesville, OK). One ml digitoxin standard solution (19.61 µg digitoxin dissolved in 1 ml HPLC-grade 100% methanol) was added to each tube and the samples were immediately vortexed for 10 s, shaken on a FastPrep shaker (MP Biomedicals, Irvine, CA) twice for 45 s at 6.5 m/s, and centrifuged for 12 min at 21,000 g. The supernatants were transferred to new labeled 1.5 ml tubes, and the extracts dried down completely in a Centrivap (Labconco, Kansas City, MO) at 30 °C, reconstituted in 100 µl absolute methanol and vortexed for approximately 30 s to dissolve the dried residue. The samples were then transferred into a syringe filter (Kinesis 13 mm, 0.45 µm; Cole-Parmer, East Bunker, CT), and pushed through into an HPLC vial with an insert (300 µl, pulled-point). Fifteen µl of the extract were injected into an Agilent 1100 series HPLC and compounds were separated on a Gemini C18 reversed phase column (5 μm, 250 mm × 10 mm, Macherey-Nagel, Düren, Germany). Cardenolides were eluted with a constant flow of 0.7 ml/min using the following gradient: 0-2 min 16% acetonitrile, 25 min 70% acetonitrile, 30-40 min 95% acetonitrile, and a 10 min post-run at 16% acetonitrile. UV absorbance spectra were recorded at 218 nm using a diode array detector (Agilent Technologies, Santa Clara, CA). Erysimoside, helveticoside, and digitoxigenin peaks were validated using commercially available standards that were run separately from the



experimental samples. The other cardenolides were identified based on the order of elution in LCMS experiments as the following retention times: cheirotoxin, rt. = 9.6 min; erysimoside, rt. = 10 min; erychroside, rt. = 10.9 min; helveticoside, rt. = 12.3 min; digitoxigenin, rt. = 16.6 min; glucodigitoxigenin, rt. = 12 min; dig-5, rt. = 13.1 min; glucodigifucoside, rt. = 13.3 min; dig-10, rt. = 14.4 min; erycordin, rt. = 10.4 min, and digitoxin, rt. = 19 min. The individual total cardenolide content was calculated based on the peak areas relative to the internal digitoxin or ouabain standard (19.6  $\mu$ g/ml) that was added to each sample.

Insect Bioassays Three days after hatching, we placed T. ni larvae individually on leaves of F2 progeny of EMS-mutagenized plants backcrossed to Elbtalaue and phenotyped by HPLC-MS. Larvae were confined on individual E. cheiranthoides leaves using  $6.5 \times 8$  cm organza bags (Fig. S2A; www.amazon.com, item B073J4RS9C). After ten days, we harvested the larvae, weighed them individually, and froze them in liquid nitrogen. We conducted the caterpillar assay with 37 mutant and 37 wildtype plants, compared the data using a two-tailed t-test, and deemed the difference significant due to P < 0.05. Experiments with P. rapae were conducted in the same manner in 15-fold replication, but we were not able to weigh the larvae because they did not survive.

Aphids were caged on *E. cheiranthoides* leaves in groups of 5 fourth-instar aphids. Cages were prepared from cut 50-ml plastic tubes (segments of 3 cm height and 3 cm diam) with a fine-mesh covered lid (Fig. S2B). After 14 days, the surviving adult aphids and nymphs were counted and frozen immediately in liquid nitrogen. We conducted the aphid assay with 16 mutant and 16 wildtype plants, compared the results using two-tailed t-tests, and deemed the difference significant if P < 0.05. Frozen caterpillar and aphid samples (10–20 mg each) were extracted and analyzed by HPLC-MS, as described for plant samples above. Cardenolide content in T. ni and M. persicae feeding on mutant plants was measured in fivefold replication and significant differences in cardenolide content were assessed using two-tailed t-tests, considering P < 0.05 to be a significant difference. Samples from both insect species were run at the same time on the same instrument.

As bodies of aphids feeding in *E. cheiranthoides* were devoid of helveticoside, we used an artificial diet assay to measure uptake of this cardenolide. Aphid artificial diet (Douglas et al. 2001) consisted of 500 mM sucrose, 150 mM amino acids (Ala, 5.7 mM; Arg, 14.3 mM; Asn, 14.3 mM; Asp, 14.3 mM; Cys, 2.7 mM; Glu, 8.4 mM; Gln, 16.5 mM; Gly, 1.2 mM; His, 8.7 mM, Ile; 8.7 mM; Leu, 8.7 mM; Lys, 8.7 mM; Met, 2.9 mM; Phe, 2.9 mM; Pro, 5.7 mM; Ser, 5.7 mM; Thr, 8.7 mM; Trp, 2.9 mM; Tyr, 0.6 mM; Val, 8.7 mM), and a mixture of essential minerals and vitamins (final diet pH 7–7.5). Helveticoside was first dissolved in absolute ethanol to make a 0.05 mg/µl stock solution and then a

100 ng/µl working solution was prepared by adding from the stock solution to the fresh diet. The diet was prepared at different concentrations of helveticoside (0, 20, 50 ng/µl). We placed a quantity of 600 µl filter-sterilized (0.2 µm) diet between two stretched layers of parafilm over the edge of the above-described cages. Forty to sixty adult aphids were placed on the underside of each diet cage and were allowed to feed for three days and then frozen immediately in liquid nitrogen for the further HPLC-MS analysis. We measured helveticoside content in aphids feeding on artificial diet with 0, 20, or 50 ng/ml helveticoside in three-fold replication at each concentration, and used Dunnett's test to confirm a significant increase in the helveticoside in aphids feeding on diet with helveticoside relative to control diet without helveticoside, considering P < 0.05 to be a significant difference.

Na<sup>+</sup>/K<sup>+</sup>-ATPase Inhibition Assay We measured porcine (Sus scrofa L) Na<sup>+</sup>/K<sup>+</sup>-ATPase activity in the presence of plant extracts, following the protocol in Züst et al. (2019), to test the inhibitory effect of the cardenolides in wildtype and 454 mutant E. cheiranthoides samples. To prepare sample extracts, we weighed 10 mg freeze-dried ground plant tissue into a screw cap tube with ~30 zirconia/silica beads (2.3 mm; BioSpec Products, Bartlesville, OK). One ml absolute methanol was added to each tube and tubes were shaken on a FastPrep shaker (MP Biomedicals, Irvine, CA) twice for 45 s at 6.5 m/s and centrifuged for 10 min at 21,000 g. Seven hundred µl supernatants were transferred to new labeled 1.5 ml microcentrifuge tubes. The extracts were dried down completely in a Centrivap (Labconco, Kansas City, MO) at 30 °C, and resuspended in 50 µL 100% dimethyl sulphoxide (DMSO) by vortexing for 20 s, sonicating in an ultrasonic bath for  $2 \times 5$  min, and briefly centrifuging (10 s) at 16,0000 g. Extracts were diluted 10-fold with deionized water (EMD Millipore, Burlington, MA) to reach a concentration of 10% DMSO. A series of six dilutions (0.3, 0.09, 0.027, 0.0081, 0.0024, 0.00073) was prepared from each fullstrength sample extract, using 10% DMSO. Six biological replicates of wildtype samples and seven biological replicates of mutated samples were distributed randomly between two 96-well plates. After further data processing compared mutant and wildtype measurements using two-tailed t-tests and deemed differences significant if P < 0.05.

We carried out enzyme assays as described in Züst et al. (2019), with ouabain standards (final concentration of 10<sup>-3</sup> to 10<sup>-8</sup> M, in 2% DMSO) included on each plate for reference. A replicated set of the dilution series, with the same reaction conditions but excluding KCl, was included for each plant sample. ATPase activity was quantified as percent control activity, by first subtracting from the reaction absorbance its appropriate background (absorbance of equivalent reaction without KCl), and then by comparison to an uninhibited



control. For each plant sample, we fitted a logistic curve to the percent enzyme activity data, as in Züst et al. (2019), except that here we used a 4-parameter function to estimate the upper and lower asymptote for each curve. We calculated cardenolide concentrations of the *E. cheiranthoides* leaf samples in terms of ouabain equivalents and compared mutant and wildtype measurements using two-tailed t-tests and deemed differences significant if P < 0.05.

Data Analysis We conducted statistical comparisons using Microsoft Excel and JMP v. 10 (www.jmp.com). In all of the box plots, the mean is indicated by an X, the median is indicated by a line, the boxes indicate the interquartile range, and the whiskers indicate the minimum and maximum. In cases where there are possible outliers, the whiskers are drawn as 1.5 times the interquartile range and possible outliers are indicated as circles. The evenness index of the cardenolide distribution was calculated using the E<sub>var</sub> method (Smith and Wilson 1996). The polarity index of mutant and wildtype E. cheiranthoides cardenolides was calculated by multiplying the proportion of each cardenolide of the total by its retention time in the HPLC-UV assay, and averaging this value across all cardenolides in the sample (Rasmann and Agrawal 2011). We conducted principal component analysis (PCA) using the following parameters in MetaboAnalyst (https://www.metaboanalyst.ca/): data filtering - interquartile range, sampling normalization - ne, data standardization none, and data scaling - none.

## Results

In an initial screen of 659 EMS-mutagenized *E. cheiranthoides* M2 plants by UPLC-MS, we were able to reliably quantify the relative abundance of ten cardenolides (Fig. 1; out of 29 that we have observed in *E. cheiranthoides*; Züst et al. 2020): digitoxigenin, four digitoxigenin glycosides (glucodigitoxigenin, glucodigifucoside, and two unknown structures labeled Dig-5 and Dig-10), a cannogenol glycoside (erycordin), and four strophanthidin glycosides (cheirotoxin, erysimoside, erychroside, and helveticoside). Dig-5 and Dig-10 have molecular weights of 537 and 521, respectively, suggesting glycosylation with glucose for Dig-5 and deoxyhexose for Dig-10, although the exact structures have not been determined.

We identified plants with divergent phenotypes for one or more cardenolides (Fig. 2a; with glucodigifucoside as an example) and subjected them to further UPLC-MS screening that resulted in five confirmed mutant lines. Mutant line 454 accumulated elevated digitoxigenin glycosides and low concentrations of cannogenol and strophanthidin glycosides (Fig. 2b). Mutants 634, 812, 826, and 894 accumulated significantly decreased amounts of most or all cardenolides (Fig. S3A-

D). Two of these mutants, 812 and 894, originated from the same M1 seed pool and may be siblings.

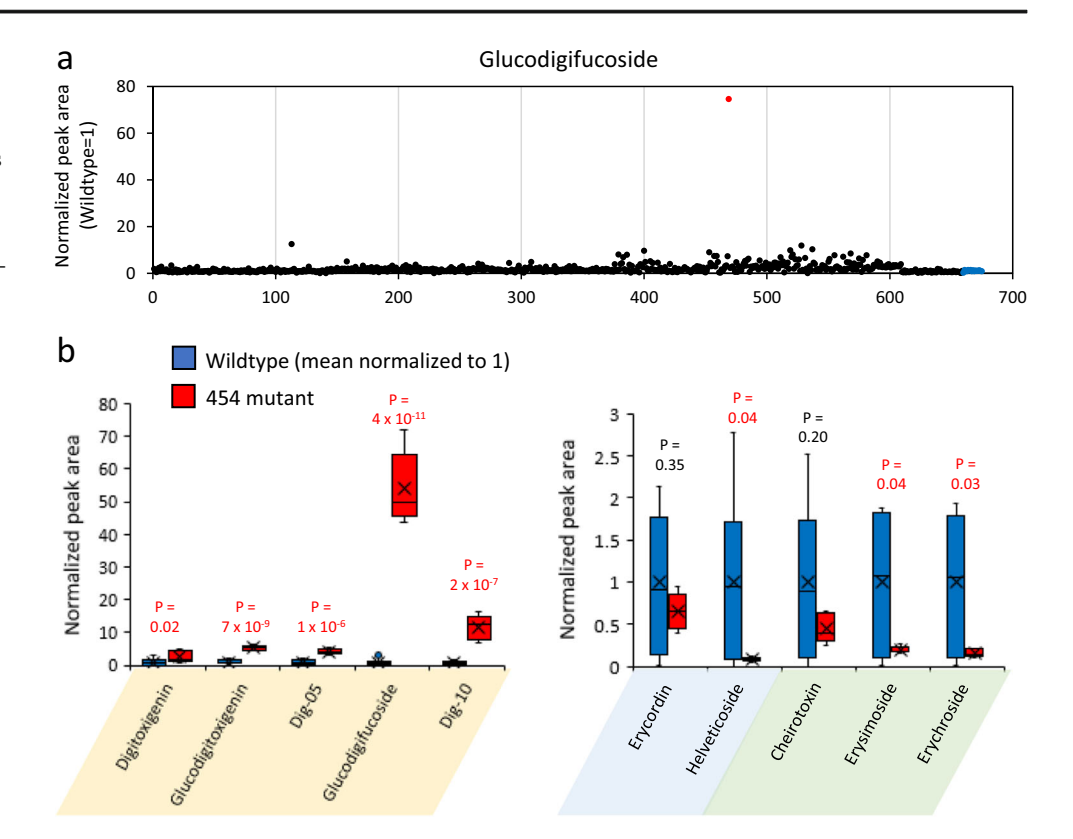
We backcrossed the 454 mutant line, which had the most distinctive phenotype, to wildtype Elbtalaue and compared the cardenolide phenotype of the F1 progeny to both parents. PCA showed that the cardenolide profile in F1 plants was similar to the wildtype parent, indicating a recessive mutation (Fig. 3a). Next, we measured cardenolides in 199 F2 progeny from a single F1 plant. Among these progeny, 155 had a wildtype cardenolide phenotype and 44 had the 454 mutant phenotype (Fig. S4), a roughly 3:1 segregation pattern that suggested a single recessive mutation. Similar to the original 454 mutant line, the 44 F2 plants with the 454 mutation had elevated digitoxigenin glycosides and decreased cannogenol and strophanthidin glycosides relative to their wildtype siblings (Fig. S4).

We mapped the genomic position of the cardenolide mutation in the 454 mutant line by bulked segregant analysis using the EMS-induced mutations in the mutant line as molecular markers (similar to Zhu et al. 2012). DNA from plants with mutant and wildtype cardenolide profiles, respectively, was pooled, subjected to Illumina sequencing, and compared to the E. cheiranthoides genome (www.erysimum.org) to identify EMS-induced polymorphisms. Plotting the frequency of the mutant alleles across the genome identified a region of ~500 kbp on chromosome 6 where the F2 plants with the mutant cardenolide phenotype were homozygous for the EMS-induced mutations (Fig. 3b). The overall frequency of EMS-induced mutant alleles across the eight E. cheiranthoides chromosomes was less than 50%, irrespective of whether the plants had the 454 mutant or wildtype cardenolide phenotype, suggesting deleterious effects from some of these unrelated mutations (Fig. 3b).

As a more quantitative assay of the cardenolide abundance in the 454 mutant and phenotypically wildtype siblings, we used HPLC-diode array detection at 218 nm, which measures absorbance of the lactone ring that is common to all of the cardenolide structures. In particular, erychroside and other strophanthidin glycosides are poorly detected in the UPLC-MS assay (Fig. 2b) relative to the UV absorption assay (Fig. 4a). Nevertheless, similar to the MS detection, the 218 nm absorption assay showed increased digitoxigenin glycosides and decreased cannogenol and strophanthidin glycosides (Fig. 4a). Notably, the 454 mutation caused a 92% decrease in erychroside. The total cardenolide UV absorbance was decreased by 66% in the 454 mutant relative to wildtype Elbtalaue (Fig. 4b). Although we found the same cardenolides in mutant and wildtype plants, the evenness of the cardenolide distribution was higher in the mutant (Fig. 4c). An index of compound polarity, calculated as HPLC retention time multiplied by relative abundance of each cardenolide (Rasmann and Agrawal 2011), was substantially higher in



Fig. 2 Mutant screen for altered cardenolide content. (a) Glucodigifucoside abundance at the first screening of 659 M2 mutant lines. Each dot represents a single plant measured by UPLC-MS. The high outlier at center-right (red dot) represents the 454 mutant line and the rightmost 16 blue dots represent wildtype Elbtalaue samples for comparison. (b) Cardenolide profile of mutant line 454, as measured by UPLC-MS, with wildtype normalize to 1 for each cardenolide. N = 5 (mutant) and 12 (wildtype). P values above bars are based on two-tailed t-tests, with P < 0.05 highlighted in red

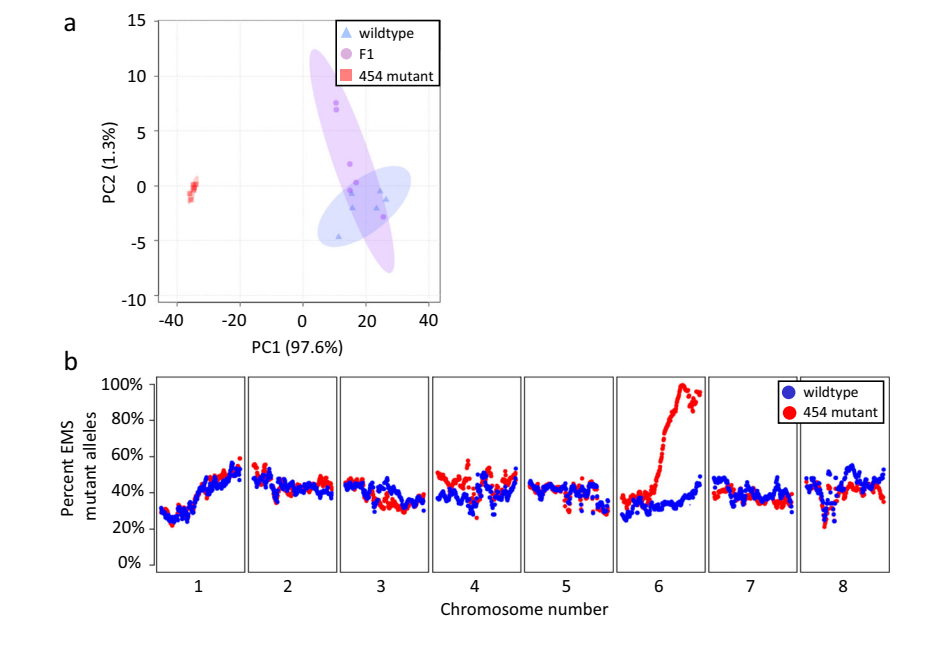


the mutant than in wildtype, indicating that the mutant cardenolide profile is less polar (Fig. 4d). With the exception of N-methylbutyl glucosinolate, which was slightly increased in the 454 mutant line, we found no significant glucosinolate changes relative to wildtype (Fig. 4e).

We next used an assay based on the inhibition of pig brain Na<sup>+</sup>/K<sup>+</sup>-ATPase (Petschenka et al. 2018) to determine

whether the 454 mutant line has altered inhibitory activity relative to its wildtype Elbtalaue progenitor. Consistent with the greater abundance of cardenolides in the wildtype samples (Fig. 4b), extracts of wildtype Elbtalaue inhibited Na<sup>+</sup>/K<sup>+</sup>-ATPase activity to a greater extent than extracts of the 454 mutant (Fig. 5a). Based on comparisons to inhibition by a dilution series of ouabain, we calculated that extracts of the

Fig. 3 Genetic properties of the 454 cardenolide mutation. (a) Principal component analysis (PCA) of the cardenolide profiles in wildtype, 454 mutant, and F1 plants (6 plants each). Colored ovals indicate 95% confidence intervals. (b) Genetic mapping by bulked segregant analysis of pooled DNA samples from 44 plants with 454 mutant cardenolide profiles and 155 plants with wildtype cardenolide profiles (shown in Fig. S3). The frequency of EMS-induced mutant alleles in the two pooled samples was plotted across the eight E. cheiranthoides chromosomes





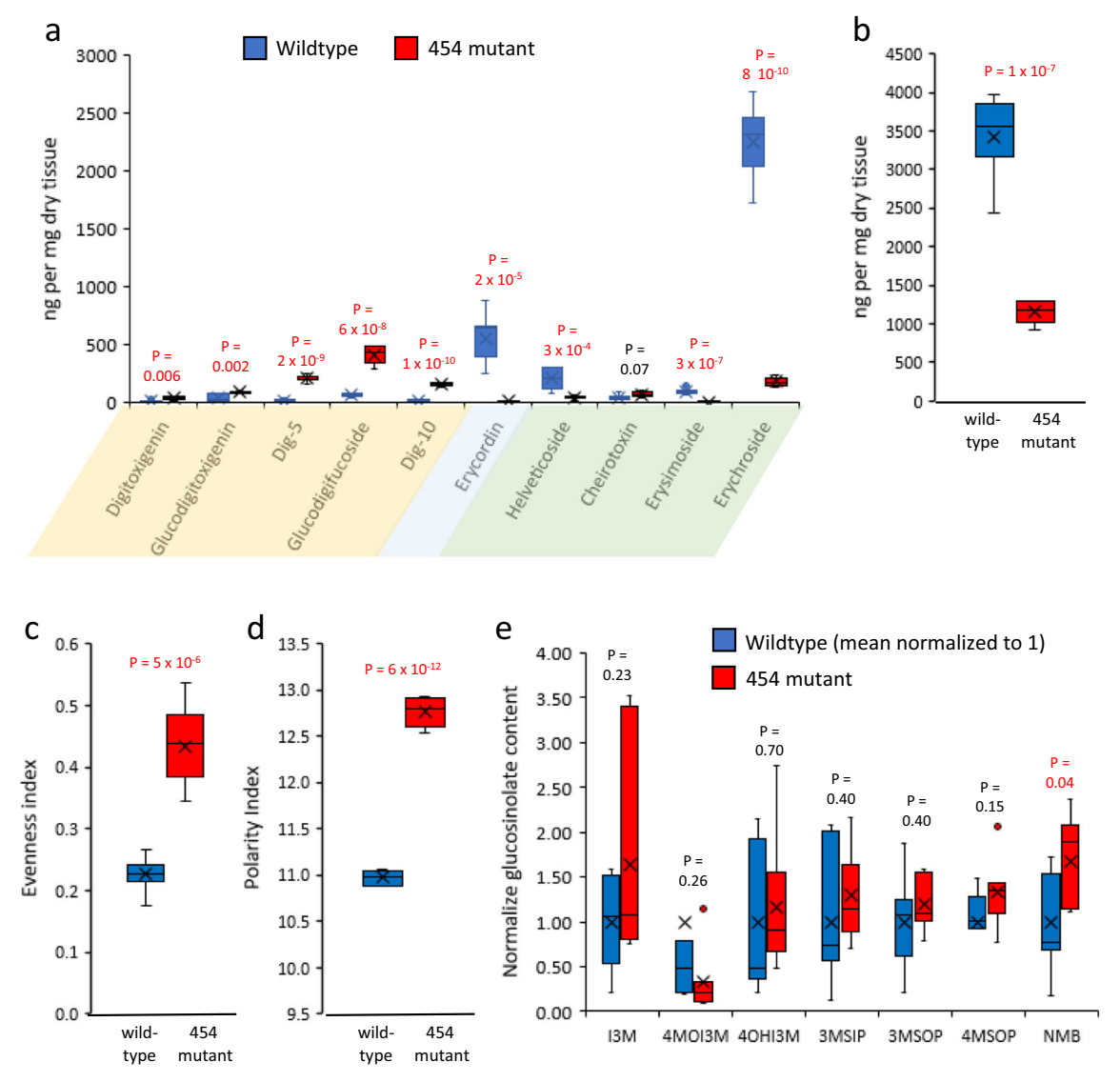


Fig. 4 Cardenolide and glucosinolate content of 454 mutant line relative to wildtype Elbtalaue. (a) Relative abundance of each individual cardenolide, and (b) total amount measured by HPLC-UV. Digitoxigenin-, cannogenol-, and strophanthidin-derived cardiac glycosides are highlighted in yellow, blue, and green, respectively. (c) Evenness of the cardenolide distribution. (d) Polarity index. (e) Relative glucosinolate content of 454 mutant line compare to wildtype measured by LCMS, with wildtype mean normalized

to one for each glucosinolate. N=7. P values above bars are based on two-tailed t-tests, with P < 0.05 highlighted in red. I3M = indol-3-ylmethyl glucosinolate, 4MOI3M = 4-methoxy-indol-3-ylmethyl glucosinolate, 4OHI3M = 4-hydroxy-indol-3-ylmethylglucosinolate, 3MSIP = 3-methylsulfinylpropyl glucosinolate, 3MSOP = 3-methylsulfonylpropyl glucosinolate, 4MSOP = 4-methylsulfonylbutyl glucosinolate, NMB = N-methylbutyl glucosinolate

454 mutant line had a 59% inhibitory activity of the Na<sup>+</sup>/K<sup>+</sup>-ATPase compared to wildtype Elbtalaue (Fig. 5b).

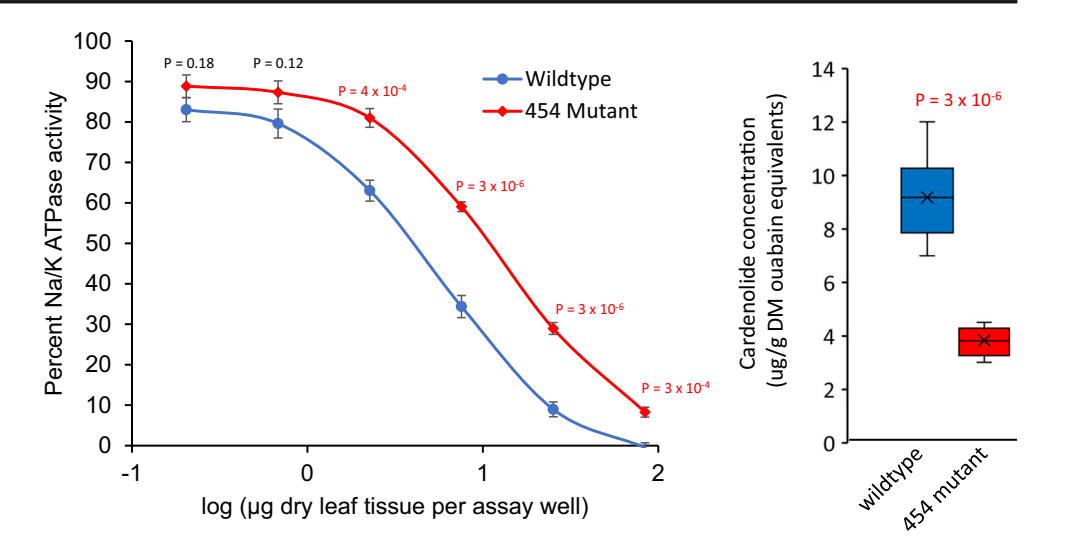
We used the segregating F2 population for bioassays with three insect herbivores, *T. ni, M. persicae*, and *P. rapae*. Relative to plants with wildtype cardenolide content, *T. ni* larvae on 454 mutant plants were 40% smaller (Fig. 6a,b), with a normal distribution of larval masses (Fig. S5), as opposed to a bimodal distribution that might arise if two mutations were segregating independently. Survival of adult *M. persicae* was not affected by the host plant genotype, but aphids produced 54% fewer progeny on the 454 mutant than on wildtype Elbtalaue (Figs. 6c and S6). Crucifer-specialist *P. rapae* larvae,

which are highly sensitive to cardenolides (Sachdev-Gupta et al. 1993), did not survive on either mutant or wildtype plants.

Both *T. ni* and *M. persicae* accumulated cardenolides in their bodies as they were feeding, with cardenolides that were more abundant in the host plants (Fig. 3a) generally also accumulating to a higher level in the insects (Fig. 6d,e). Dig-5, digitoxigenin, and erycordin were not reliably detected in the insect bodies and were therefore not quantified. In samples that were run at the same time on the same instrument, we found that most of the measured cardenolides were more abundant in *T. ni* larvae than in *M. persicae* (Table 1). However, erysimoside and erychroside were more abundant

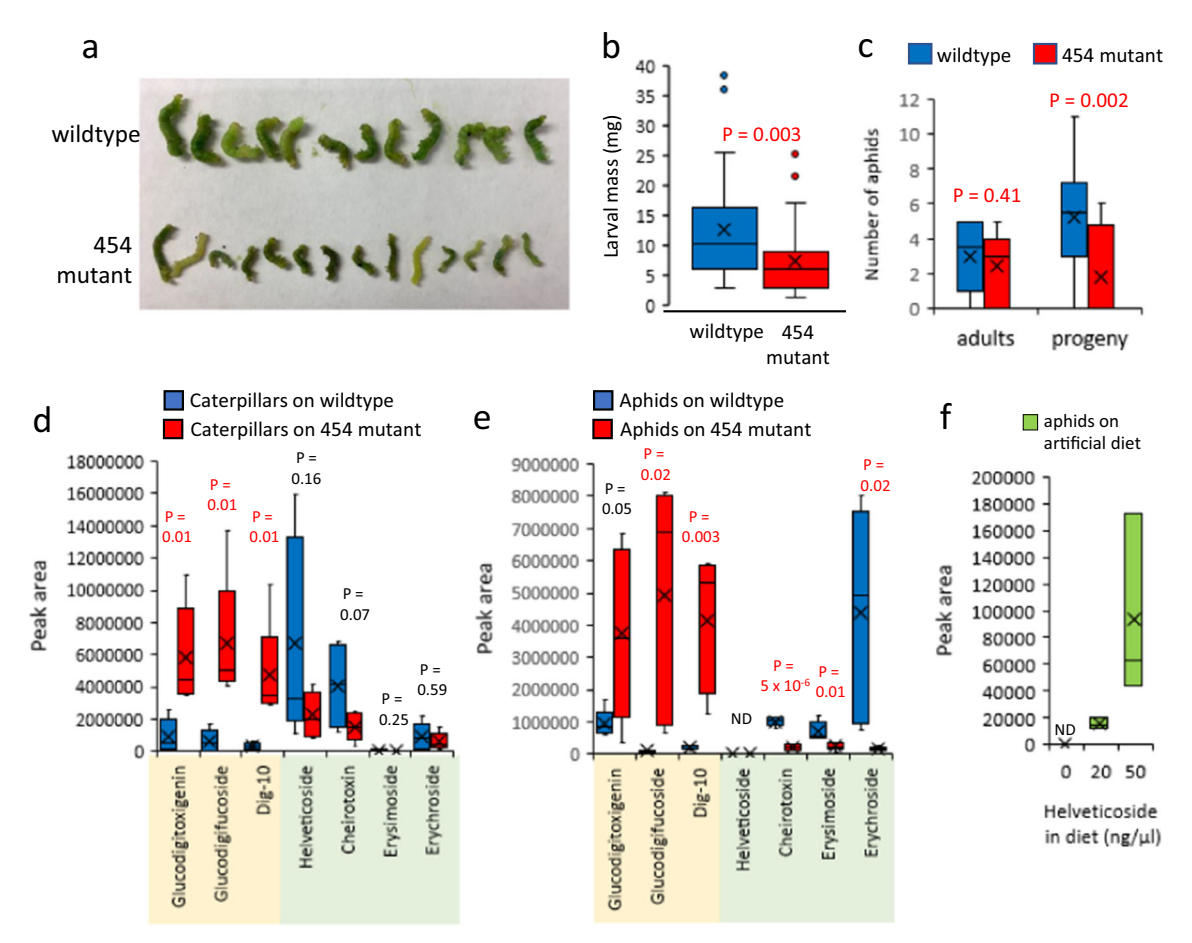


Fig. 5 Inhibition of porcine  $\mathrm{Na}^+/\mathrm{K}^+$  ATPase. (a) Percent inhibition by dilutions of extracts of wildtype Elbtalaue and 454 mutant *E. cheiranthoides*. (b) Amount of inhibitory activity expressed as an equivalent amount of ouabain. N=7 (mutant samples), N=6 (wildtype samples), P values were determined with two-tailed t-tests, with P < 0.05 highlighted in red



in aphids than in caterpillars when feeding on wildtype Elbtalaue. Helveticoside was not detected in aphids feeding on either wildtype or mutant *E. cheiranthoides* (Fig. 6e). However, when we added helveticoside to aphid artificial diet

at a concentration similar to that found in *E. cheiranthoides* leaves, we found helveticoside in the aphid bodies by UPLC-MS (Fig. 6f), suggesting that helveticoside is not present in the phloem.



**Fig. 6** Insect growth on 454 mutant plants and segregating wildtype progeny from a backcross to wildtype Elbtalaue. (a) Photograph of a subset of the *Trichoplusia ni* larvae after 10 days of feeding. (b) T. ni larval mass, N = 37. (c) Number of surviving adult aphids and progeny after two weeks feeding. N = 16. Cardiac glycoside content in (d) T. ni

caterpillars and (e) *M. persicae* feeding on sibling plants with wildtype and 454 mutant cardenolide content. N = 5. P values above bars are based on two-tailed t-tests, with P < 0.05 highlighted in red. (F) Helveticoside content in M. persicae feeding from artificial diet with helveticoside. N = 3. ND = not detected



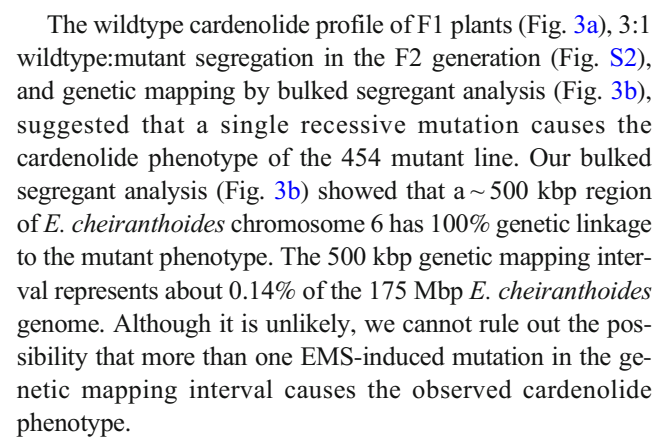
**Table 1** Cardenolide abundance in insects feeding on *E. cheiranthoides*, peak area/mg in *M. persicae* relative to *T. ni* 

	M. persicae/T. ni ratio	
	Wildtype	454 Mutant
Glucodigitoxigenin	1.00	0.64
Glucodigifucoside	0.16	0.74
Dig-10	0.59	0.88
Erycordin	0.23	0.21
Helveticoside	0.00	0.00
Cheirotoxin	0.25	0.13
Erysimoside	11.34	10.79
Erychroside	4.80	0.27

### **Discussion**

The molecular characterization of mutations and natural variation can facilitate research on the defensive functions of plant specialized metabolites, which are often produced as classes of compounds with similar chemical structures and target sites in insect herbivores. Until fairly recently, such experiments were only feasible with classes of defensive metabolites that are present in well-studied model systems, such as glucosinolates in *A. thaliana*, benzoxazinoids in *Zea mays* L (Poaceae), and glycoalkaloids in *Solanum lycopersicum* L (Solanaceae). However, advances in genome sequencing and molecular methods have made it feasible to initiate such research using non-model systems such as cardenolide production in *E. cheiranthoides*.

In a screen of EMS-mutagenized E. cheiranthoides var. Elbtalaue, we identified mutant line 454, which had a dramatic shift in its cardenolide profile. This shift resulted in a 66% decrease in total cardenolide content that was due to lower accumulation of cannogenol and strophanthidin glycosides, which was partially compensated for by an increase in digitoxigenin glycosides (Fig. 4b). Consistent with the decrease in total cardenolide content, extracts of the 454 mutant inhibited the highly sensitive porcine Na<sup>+</sup>/K<sup>+</sup>-ATPase activity 59% less than extracts of wildtype Elbtalaue (Fig. 5), indicating that the different E. cheiranthoides cardenolides do not fundamentally differ in their inhibitory activity in this in vitro enzyme assay. This observation is consistent with a survey of 28 Erysimum species, where despite a vast diversity in cardenolide compounds, the total cardenolide HPLC-MS peak area was strongly correlated with in vitro Na<sup>+</sup>/K<sup>+</sup>-ATPase inhibition (r = 0.95, p < 0.001; Züst et al. 2020). The shift in cardenolide profile of the 454 mutant line also resulted in a more even cardenolide distribution (Fig. 4c), which was largely due to a greater than 90% decrease in the amount of erychroside, a polar strophanthidin glycoside that is the most abundant cardenolide in wildtype E. cheiranthoides.



Our EMS mutagenesis induced numerous mutations in the E. cheiranthoides genome. It is likely that most of these do not have phenotypic effects. However, the mutant alleles for many markers were present at less than 50% abundance, an effect that is particularly noticeable at the left side of chromosomes 1 and 6 in Fig. 3b. This observation suggests that some of these unlinked mutations have deleterious effects on E. cheiranthoides growth and survival, irrespective of the cardenolide profile. Similarly, additional mutations in the 454 line might affect our assays of insect growth, Na<sup>+</sup>/K<sup>+</sup> ATPase inhibition, and glucosinolates. However, we conducted these assays with a segregating F2 population that was separated as 454 mutant or wildtype based on the cardenolide profile. Therefore, genetic segregation would average out the effects of mutations that are not located near the cardenolide mutation on chromosome 6. Additionally, the normal distribution of caterpillar weights on the F2 plants (Fig. S5) is consistent with a single locus rather than two genetically unliked loci affecting caterpillar growth.

Structural comparisons suggest that digitoxigenin, likely the most basal of the three genins, would be converted to cannogenol by a hydroxylase, possibly a cytochrome P450 (Fig. 1). The cannogenol and strophanthidin classes of cardenolides could be eliminated by a knockout mutation of such an enzyme. However, it is also possible that a regulatory mutation reduces conversion of digitoxigenin to cannogenol and strophanthidin. For instance, in A. thaliana indole glucosinolate accumulation can be reduced by both mutations in biosynthetic genes, e.g. cytochrome P450 genes, CYP79B and CY79B3 (Zhao et al. 2002), and by mutations in regulatory genes, e.g. the transcription factors MYB34, MYB51, and MYB122 (Frerigmann and Gigolashvili 2014). Map-based cloning of the 454 mutation will be required to determine whether a biosynthetic or regulatory gene of the cardenolide pathway in E. cheiranthoides is affected. Other E. cheiranthoides mutations, which caused more uniform decreases in total cardenolide content (Fig. S2A-D), may affect earlier steps in the biosynthetic pathway and are worthwhile targets for future studies.



Although we hypothesize that a change in the cardenolide profile changes E. cheiranthoides herbivore resistance, we cannot rule out the possibility that direct or indirect regulatory effects on other E. cheiranthoides defenses affect resistance to T. ni and M. persicae feeding. For instance, the increase in the structurally uncharacterized N-methylbutyl glucosinolate in the mutant line (Fig. 4e) may have contributed to enhanced insect resistance in the 454 mutant. However, M. persicae is impervious to methionine-derived aliphatic glucosinolates (Kim et al. 2008) and a total loss of aliphatic glucosinolates in A. thaliana was required to cause a 50% increase in T. ni growth (Müller et al. 2010). The increase in I3M and decrease in 4MOI3M in the 454 mutant relative to wildtype were not significant in our assays (Fig. 4e). In any case, we do not expect that such glucosinolate changes would cause the observed increase T. ni and M. persicae resistance. Experiments with Arabidopsis showed that T. ni larval weight gain was not significantly affected by indole glucosinolate mutations (Müller et al. 2010) and the observed decrease in 4MOI3M would be expected to increase M. persicae progeny production (Kim and Jander 2007), the opposite of what we observed with the 454 mutant line (Fig. 6c).

Three scenarios may account for the reduced insect growth on the 454 mutant line despite the lower total amounts of cardenolides in these plants: (i) in contrast to the pig enzyme, insect enzymes may be more sensitive to digitoxigenin glycosides; (ii) there is differential uptake of cardenolides in insects; or (iii) the two insect species can detoxify or excrete polar cardenolides more easily than apolar cardenolides. Although we currently lack information on the specific Na<sup>+</sup>/K<sup>+</sup>-ATPase sensitivities of T. ni and M. persicae, experiments with pig, Drosophila, and non-specialist lepidopteran species showed similar cardenolide sensitivities (Karageorgi et al. 2019), making the first scenario perhaps less likely. After ingestion, cardenolides must cross multiple membranes to get to their target sites, which are specifically located within nerve cells. Therefore, the polarity of individual cardenolides, which affects their solubility in aqueous solutions and lipid membranes, could influence their in vivo toxicity. Previous research with M. persicae and three other aphid species feeding on Asclepias spp. (milkweed) showed that the aphids accumulated predominantly apolar cardenolides in their bodies while they could excrete polar cardenolides with their honeydew (Züst and Agrawal 2015), suggesting that uptake and excretion may play an important role in our study as well. Erychroside, the most abundant cardenolide in wildtype E. cheiranthoides, is the third-most polar cardenolide produced by this species and, despite its high abundance, both T. ni and M. persicae accumulated this compound at markedly lower proportions relative to other cardenolides. This suggests that both herbivores were able to prevent uptake, partially detoxify, or excrete this compound. In T. ni, this detoxification may have involved cleaving of the outer xylose sugar, resulting in an increased accumulation of helyeticoside (Fig. 6d), which was found to have no deterrent effects on the otherwise highly cardenolide-susceptible P. rapae (Renwick et al. 1989; Sachdev-Gupta et al. 1990). Aphids may have been able to rapidly excrete erychroside without ever taking it up into their body cavity, although further evaluation of cardenolide profiles in aphid honeydew will be necessary to confirm this. Assuming that the most abundant cardenolide compound of wildtype plants is largely ineffective against these insect herbivores, the shift to a higher proportion of digitoxigenin cardenolides and a more apolar profile in the 454 mutant line may therefore have increased the cardenolide load of both herbivores despite lower total amounts in the plant. This increased cardenolide load could then have caused a reduction in performance due to direct toxicity or by requiring larger investment into general detoxification mechanisms.

Differential accumulation of E. cheiranthoides cardenolides by the two insect species (Table 1, Fig. 6d,e) may at least in part be reflective of their feeding styles. Whereas T. ni larvae consume leaf tissue, M. persicae feed exclusively from the phloem. Higher accumulation of erysimoside by M. persicae may indicate that this cardenolide is relatively more abundant in the phloem than in the leaf as a whole. Conversely, the complete absence of helveticoside in aphids feeding from both wildtype and mutant E. cheiranthoides suggests that this cardenolide may be low or absent in the phloem. When we added helveticoside to aphid artificial diet at concentrations comparable to those found in E. cheiranthoides leaves (>20 ng/mg wet weight in wildtype Elbtalaue), we were able to detect helveticoside in the aphid bodies (Fig. 6f). Therefore, the absence of helveticoside in M. persicae feeding on E. cheiranthoides is likely not due to degradation of helveticoside by the aphids or inhibited uptake from the aphid gut. Helveticoside is unique among E. cheiranthoides cardenolides as its glycoside moiety consists solely of a digitoxose sugar (Fig. 1). In a large comparison of cardenolide uptake by Digitalis lanata cells, Christmann et al. (1993) concluded that cardenolides with terminal glucose sugars are phloem mobile, whereas those with terminal digitoxose sugars are not. Consistent with these Digitalis experiments, our aphid uptake assays indicate a lack of phloem mobility for helveticoside, but also suggest that xylose, the terminal sugar of erychroside, can enable cardenolide phloem mobility as well.

The 454 mutant line was more resistant against insect herbivores from two different feeding guilds than the wildtype plant, despite producing an overall lower quantity of cardenolide defenses. At first glance, it thus appears that the 454 mutant line should represent a superior evolutionary strategy that should quickly outcompete the wildtype if it ever arose naturally. However, to fully understand the evolutionary drivers of these defense phenotypes, it will be essential to evaluate plant performance in the native habitat of



E. cheiranthoides, as we may well be missing important constraints or antagonists that favor the wildtype phenotype. For example, larger mammalian herbivores may respond more to the bitter taste of cardenolides rather than their toxicity, in which case it may be more beneficial for plants to produce large quantities of a putatively 'cheaper' compound. Yet even without knowing all evolutionary drivers of the E. cheiranthoides defense phenotype, we can nonetheless conclude that a more diverse mixture of cardenolides serves to cope with the diversity of antagonists that threaten this plant.

Our results demonstrate the feasibility of using a mutagenesis approach to study the in vivo function of cardenolides in defense against insect herbivores. Isolation of additional mutations affecting the accumulation of individual cardenolides will enable research on their in vivo functions in plant defense. Moreover, genetic mapping of such mutations will make it possible to identify genes in the cardenolide biosynthetic pathway, which remains mostly unidentified in *E. cheiranthoides* and other cardenolide-producing plant species.

**Supplementary Information** The online version contains supplementary material available at (https://doi.org/10.1007/s10886-020-01225-y).

**Acknowledgements** We thank the Biotechnology Resource Center and Bioinformatics Facility at Cornell University for assistance in developing data analysis scripts.

**Funding** This research was funded by US National Science Foundation awards 1907491 to AAA and 1645256 to GJ and AAA, Swiss National Science Foundation grant PZ00P3-161472 to TZ, and a Triad Foundation grant to GJ.

# References

- Agrawal AA, Petschenka G, Bingham RA, Weber MG, Rasmann S (2012) Toxic cardenolides: chemical ecology and coevolution of specialized plant-herbivore interactions. New Phytol 194:28–45. https://doi.org/10.1111/j.1469-8137.2011.04049.x
- Berenbaum MR, Nitao JK, Zangerl AR (1991) Adaptive significance of furanocoumarin diversity in *Pastinaca sativa* (Apiaceae). J Chem Ecol 17:207–215. https://doi.org/10.1007/BF00994434
- Christmann J, Kreis W, Reinhard E (1993) Uptake, transport and storage of cardenolides in foxglove cardenolide sinks and occurrence of cardenolides in the sieve tubes of *Digitalis lanata*. Botanica Acta 106:419–427. https://doi.org/10.1111/j.1438-8677.1993.tb00769.x
- Dimock MB, Renwick JA, Radke CD, Sachdev-Gupta K (1991) Chemical constituents of an unacceptable crucifer, *Erysimum cheiranthoides*, deter feeding by *Pieris rapae*. J Chem Ecol 17: 525–533. https://doi.org/10.1007/BF00982123
- Douglas AE, Minto LB, Wilkinson TL (2001) Quantifying nutrient production by the microbial symbionts in an aphid. J Exp Biol 204: 349–358

- Dzimiri N, Fricke U, Klaus W (1987) Influence of derivation on the lipophilicity and inhibitory actions of cardiac glycosides on myocardial Na+-K+-ATPase. Br J Pharmacol 91:31–38. https://doi.org/10.1111/j.1476-5381.1987.tb08980.x
- Fahey JW, Zalcmann AT, Talalay P (2001) The chemical diversity and distribution of glucosinolates and isothiocyanates among plants. Phytochemistry 56:5–51
- Farr CD, Burd C, Tabet MR, Wang X, Welsh WJ, Ball WJ Jr (2002)
  Three-dimensional quantitative structure-activity relationship study
  of the inhibition of Na(+),K(+)-ATPase by cardiotonic steroids
  using comparative molecular field analysis. Biochemistry 41:
  1137–1148. https://doi.org/10.1021/bi011511g
- Frerigmann H, Gigolashvili T (2014) MYB34, MYB51, and MYB122 distinctly regulate indolic glucosinolate biosynthesis in *Arabidopsis thaliana*. Mol plant 7:814–828. https://doi.org/10.1093/mp/ssu004
- Groen SC, LaPlante ER, Alexandre NM, Agrawal AA, Dobler S, Whiteman NK (2017) Multidrug transporters and organic anion transporting polypeptides protect insects against the toxic effects of cardenolides Insect. Biochem Mol Biol 81:51–61. https://doi. org/10.1016/j.ibmb.2016.12.008
- Jander G, Baerson SR, Hudak JA, Gonzalez KA, Gruys KJ, Last RL (2003) Ethylmethanesulfonate saturation mutagenesis in Arabidopsis to determine frequency of herbicide resistance. Plant Physiol 131:139–146
- Karageorgi M et al (2019) Genome editing retraces the evolution of toxin resistance in the monarch butterfly. Nature 574:409–412. https://doi. org/10.1038/s41586-019-1610-8
- Kim JH, Jander G (2007) *Myzus persicae* (green peach aphid) feeding on Arabidopsis induces the formation of a deterrent indole glucosinolate. Plant J 49:1008–1019
- Kim JH, Lee BW, Schroeder FC, Jander G (2008) Identification of indole glucosinolate breakdown products with antifeedant effects on Myzus persicae (green peach aphid). Plant J 54:1015–1026
- Li H (2011) A statistical framework for SNP calling, mutation discovery, association mapping and population genetical parameter estimation from sequencing data. Bioinformatics 27:2987–2993. https://doi.org/10.1093/bioinformatics/btr509
- Li H, Durbin R (2009) Fast and accurate short read alignment with Burrows-Wheeler transform. Bioinformatics 25:1754–1760. https://doi.org/10.1093/bioinformatics/btp324
- Li H et al (2009) The sequence alignment/map format and SAMtools. Bioinformatics 25:2078–2079. https://doi.org/10.1093/bioinformatics/btp352
- Müller R, De Vos M, Sun JY, Sønderby IE, Halkier BA, Wittstock U, Jander G (2010) Differential effects of indole and aliphatic glucosinolates on lepidopteran herbivores. J Chem Ecol 36:905–913
- Paula S, Tabet MR, Ball WJ Jr (2005) Interactions between cardiac glycosides and sodium/potassium-ATPase: three-dimensional structure-activity relationship models for ligand binding to the E2-pi form of the enzyme versus activity inhibition. Biochemistry 44:498–510. https://doi.org/10.1021/bi048680w
- Petschenka G, Fei CS, Araya JJ, Schroder S, Timmermann BN, Agrawal AA (2018) Relative selectivity of plant cardenolides for Na(+)/K(+)-ATPases from the monarch butterfly and non-resistant insects. Front Plant Sci 9:1424. https://doi.org/10.3389/fpls.2018.01424
- Petschenka G, Pick C, Wagschal V, Dobler S (2013) Functional evidence for physiological mechanisms to circumvent neurotoxicity of cardenolides in an adapted and a non-adapted hawk-moth species. Proc Biol Sci 280:20123089. https://doi.org/10.1098/rspb.2012.3089
- R Core Team (2020) R: A language and environment for statistical computing. Foundation for Statistical Computing. https://www.R-project.org/. 2020
- Ramsey JS, Elzinga DA, Sarkar P, Xin Y-R, Ghanim M, Jander G (2014) Adaptation to nicotine feeding in *Myzus persicae*. J Chem Ecol 40: 869–877. https://doi.org/10.1007/s10886-014-0482-5



- Ramsey JS et al (2007) Genomic resources for Myzus persicae: EST sequencing, SNP identification, and microarray design. BMC Genomics 8:423
- Rasmann S, Agrawal AA (2011) Latitudinal patterns in plant defense: evolution of cardenolides, their toxicity and induction following herbivory. Ecol Lett 14:476–483. https://doi.org/10.1111/j.1461-0248.2011.01609.x
- Renwick JA, Radke CD, Sachdev-Gupta K (1989) Chemical constituents of Erysimum cheiranthoides deterring oviposition by the cabbage butterfly Pieris rapae. J Chem Ecol 15:2161–2169. https://doi.org/ 10.1007/BF01014106
- Sachdev-Gupta K, Radke C, Renwick JA, Dimock MB (1993) Cardenolides from *Erysimum cheiranthoides*: Feeding deterrents to *Pieris rapae* larvae. J Chem Ecol 19:1355–1369. https://doi.org/ 10.1007/BF00984881
- Sachdev-Gupta K, Renwick JA, Radke CD (1990) Isolation and identification of oviposition deterrents to cabbage butterfly, *Pieris rapae*, from *Erysimum cheiranthoides*. J Chem Ecol 16:1059–1067. https://doi.org/10.1007/BF01021010
- Salazar D, Lokvam J, Mesones I, Vasquez Pilco M, Ayarza Zuniga JM, de Valpine P, PVA F (2018) Origin and maintenance of chemical diversity in a species-rich tropical tree lineage. Nat Ecol Evol 2:983– 990. https://doi.org/10.1038/s41559-018-0552-0
- Schonfeld W et al (1985) The lead structure in cardiac glycosides is 5 beta, 14 beta-androstane-3 beta 14-diol Naunyn Schmiedebergs. Arch Pharmacol 329:414–426. https://doi.org/10.1007/bf00496377
- Smith B, Wilson JB (1996) A consumer's guide to evenness indices Oikos 76:70-82 doi:Doi. https://doi.org/10.2307/3545749

- Wickham H, Francois R, Henry L, Müller K (2020) Dplyr: a grammar of data manipulation. https://CRAN.R-project.org/package=dplyr
- Wittstock U, Agerbirk N, Stauber EJ, Olsen CE, Hippler M, Mitchell-Olds T, Gershenzon J, Vogel H (2004) Successful herbivore attack due to metabolic diversion of a plant chemical defense. Proc Natl Acad Sci U S A 101:4859–4864
- Zhao Y et al (2002) Trp-dependent auxin biosynthesis in Arabidopsis: involvement of cytochrome P450s CYP79B2 and CYP79B3. Genes Dev 16:3100–3112
- Zhu Y, Mang HG, Sun Q, Qian J, Hipps A, Hua J (2012) Gene discovery using mutagen-induced polymorphisms and deep sequencing: application to plant disease resistance. Genetics 192:139–146. https://doi. org/10.1534/genetics.112.141986
- Züst T, Agrawal AA (2015) Population growth and sequestration of plant toxins along a gradient of specialization in four aphid species on the common milkweed Asclepias syriaca. Functional Ecology 186:E1– E15
- Züst T, Mirzaei M, Jander G (2018) Erysimum cheiranthoides, an ecological research system with potential as a genetic and genomic model for studying cardiac glycoside biosynthesis. Phytochem Rev 17:1239–1251
- Züst T, Petschenka G, Hastings AP, Agrawal AA (2019) Toxicity of milkweed leaves and latex: Chromatographic quantification versus biological activity of cardenolides in 16 Asclepias species. J Chem Ecol 45:50–60. https://doi.org/10.1007/s10886-018-1040-3
- Züst T et al (2020) Rapid and independent evolution of ancestral and novel defenses in a genus of toxic plants (*Erysimum*, Brassicaceae). eLife 9:e51712. https://doi.org/10.7554/eLife.51712

